Contribution de la simulation numérique multiphysique CFD à la réduction des émissions de polluants d'appareils de chauffage domestique : application à un poêle à granulés.

Contribution of multiphysics CFD simulation to the reduction of pollutant emissions from domestic heating appliances: application to a pellet stove.

Alexandre BRICLOT[1,2], Marta PALMA[3], Andrea TEZZA[3], David FREZZATO[2], Fabio SIMONETTO[2,3], Jaona Harifidy RANDRIANALISOA[1*]

[1]ITheMM UR7548, Université de Reims Champagne-Ardenne
UFR SEN, Campus Moulin de la Housse, 51100 Reims (France)
[2]Invicta
57 rue des Manises - 08440 Vivier-au-Court (France)
[3]Caminetti Montegrappa,
Via Annibale de Bassano, 7/9, 36020 Pove del Grappa (Italy)
[*](Corresponding author: jaona.randrianalisoa@univ-reims.fr)

Résumé - Les appareils domestiques de combustion de la biomasse, comme les poêles à granulés, sont des sources de chauffage importantes pour de nombreux ménages européens mais sont sources de polluants tels que le monoxyde de carbone, les oxydes d'azote et les particules fines. Afin de réduire ces émissions, un modèle numérique multiphysique 3D d'un poêle à granulés a été développé avec le logiciel ANSYS Fluent. Une comparaison avec les concentrations expérimentales de gaz à la sortie du poêle, les températures de flamme à différentes hauteurs dans l'appareil et la puissance du poêle a démontré la pertinence du modèle.

Abstract - Domestic biomass combustion devices, such as pellet stoves, are important heating sources for many European households but are source of pollutants such as carbon monoxide, nitrogen oxides and fine particle matter. To reduce the emission of pollutants, a 3D multiphysics numerical model of an existing pellet stove was developed using the ANSYS Fluent software. A comparison with relevant experimental gas concentrations at the stove outlet, flame temperatures at different heights within the appliance and the stove power has demonstrated the suitability of the model.

Nomenclature

C_p	Specific heat capacity, $J.kg^{-1}.K^{-1}$
g	Gravitational acceleration, $m.s^{-2}$
I	Radiance, $W.m^{-2}.sr^{-1}$
k	Thermal conductivity, $W.m^{-1}.K^{-1}$
n	Refractive index
N_i	Number of bands
p	Pressure, Pa
$\boldsymbol{q_R}$	Radiative heat flux, $W.m^{-2}$
$\boldsymbol{r}$	Position
$\boldsymbol{s}$	Direction
S	Heat source, $W.m^{-3}$
T	Temperature, K
$\boldsymbol{u}$	Velocity, $m.s^{-1}$
x	Combustion product
X	Mole fraction
Greek symbols	
η	Wave number, cm^{-1}
κ	Absorption coefficient, m^{-1}
ρ	Density, $kg.m^{-3}$
τ	Shear stress, Pa
φ	Char oxidation parameter
Ω	Solid angle, sr
Index and exponent	
i	Band number
h	Homogeneous
dry	Drying
pyro	Pyrolysis
char	Char oxidation

https://doi.org/10.25855/SFT2025-106

1. Introduction

In order to improve the air quality and comply with French and European standards, it is of major importance to reduce the emission of pollutants of domestic heating appliances, especially carbon monoxide (CO), nitrogen oxides (NOx) and particulate matter (PM). In this case, Computational Fluid Dynamics (CFD) proves to be a valuable tool to optimize the operating conditions and reduce the cost of development compared to a classical experimental approach.

Gómez *et al.* [1] developed a transient model with ANSYS Fluent to study the compaction of packed bed and the combustion of biomass taking into account several physics such as drying, pyrolysis and char oxidation that are not natively implemented into Fluent. They investigated the impact of air flow rate on temperatures, front thickness and bed height. Their numerical simulations showed acceptable results compared to experiments.

Detailed mechanism of combustion in a wood log stove, including more than 600 species and 4700 reactions, was studied by Darido *et al.* [2] using an Equivalent Reactor Network approach with the aim of predicting the pollutant emissions. Due to the complexity of this study, the heat and fluid flow models were simplified. Their simulations showed a good agreement with the experimental concentrations of pollutants (CO, CO_2 and NOx). However, they did not take into account the effects of radiation, nor the formation of soot.

Compared to the existing studies, this work aims to develop an engineering solution to predict the formation of pollutants including carbon monoxide and dioxide, nitrogen oxides and soot with a focus on detailed heat and fluid flow and a simplified chemical reaction mechanism. It also includes multi-band radiation model to take into account the spectral dependence of the radiative properties of the combustion products. The formation of soot and NOx are also considered.

2. Numerical model

2.1. Geometry & Mesh

A 3D numerical geometry of the commercial AVALON2 pellet stove (Figure 1) by Caminetti Montegrappa (Invicta Group) was developed to accurately model the combustion of pellets. Pellets are modeled as finite length cylinders and are placed with random orientation into two layers within the crucible: carbonized pellets (diameter of 4 mm and length comprised between 3 and 18 mm) at the bottom of the crucible and fresh pellets (diameter of 6 mm and length comprised between 5 and 25 mm) on top. The dimensions of the combustion chamber are 156×300×450 mm^3. At nominal operating conditions, the consumption rate of pellets, output power and efficiency are respectively 2.13 kg/h, 9.1 kW and 89.5%.

The 3D numerical model was discretized into 12 million poly-hexcore cells with a maximum cell length of 6 mm. Regions of interest (i.e. pellets and fluid in the crucible and above), where the temperature gradients are expected to be high were refined to 0.75 mm. The near-wall regions of the stove were also refined using inflations of 5 layers. The average orthogonal quality of the cells is 0.96 with a minimum of 0.2.

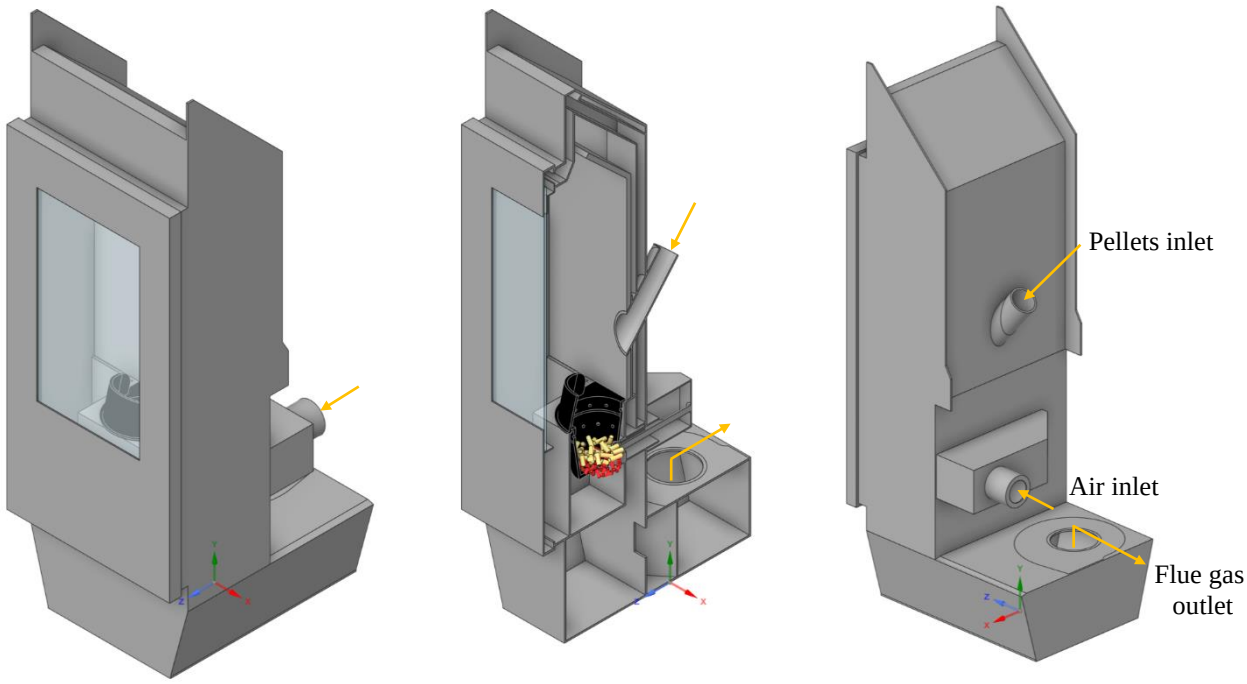

Figure 1: Geometry of the pellet stove with pellets in the crucible

2.2. Model description

Even though the combustion of biomass is a transient phenomenon, the combustion in pellet stoves can be approximated as a steady-state problem as the pellets are continuously fed into the crucible.

The fluid flow in such conditions is turbulent and is therefore solved using the Realizable k-ε model with Enhanced Wall Treatment (EWT) to better model the flow near the walls. All the thermophysical properties are temperature-dependent due to high temperature gradients in the stove. Therefore, the Navier-Stokes equations can be written [3]:

$$\boldsymbol{\nabla}.(\rho \boldsymbol{u}) = 0 \tag{1}$$

$$\boldsymbol{\nabla}.(\rho \boldsymbol{u}\boldsymbol{u}) = -\boldsymbol{\nabla} p + \boldsymbol{\nabla}.(\bar{\bar{\boldsymbol{\tau}}}) + \rho \boldsymbol{g} \tag{2}$$

where ρ and p denote the density and the pressure of the fluid while $\boldsymbol{u}$ is the velocity of the fluid, $\boldsymbol{g}$ is the gravitational acceleration and $\bar{\bar{\boldsymbol{\tau}}}$ is the stress tensor. At the inlet, a mass flowrate is imposed, corresponding to the value experimentally determined (See section 3.2) while a pressure condition is applied at the outlet. Additionally, mass sources are applied at the surface of the pellets to simulate drying, pyrolysis and char oxidation.

Furthermore, the fluid and solid energy equations are solved [3]:

$$\boldsymbol{\nabla}.\left(\boldsymbol{u}\rho_f C_p T_f\right) = \boldsymbol{\nabla}.\left(k_f \boldsymbol{\nabla} T_f\right) - \boldsymbol{\nabla}.\boldsymbol{q_R} + S_h \tag{3}$$

$$\boldsymbol{\nabla}.(k_s \boldsymbol{\nabla} T_s) + S_{dry} + S_{pyro} + S_{char} = 0 \tag{4}$$

where C_p, k, T, S and q_R respectively denote the specific heat capacity, thermal conductivity, temperature, heat sources and the radiative heat flux while the subscripts f, s, h, dry, pyro and

char denote fluid, solid, homogeneous, drying, pyrolysis and char oxidation. In the fluid domains, the heat sources come from exothermic homogeneous reactions while in the solid pellets, they arise from either endothermic (drying and pyrolysis) or exothermic (char oxidation) reactions. Regarding the thermal boundary conditions, all external surfaces are exposed to the ambient air and are subject to both natural convection with a variable heat transfer coefficient determined by Nusselt correlations [4], and radiation with a constant emissivity of 0.8.

During drying and pyrolysis, a total of 8 species are fed into the domain: methane CH_4, benzene C_6H_6, ethane C_2H_6, ethylene C_2H_4, carbon monoxide CO, hydrogen H_2, carbon dioxide CO_2 and water vapor H_2O. Their mass fractions are experimentally determined in section 3.1. Combustion of these species is modeled by a two-step mechanism of 6 homogeneous oxidation reactions and the Water-Gas Shift Reaction (WGSR) [1,5]:

$$\mathrm{CH_4} + \frac{3}{2}\,\mathrm{O_2} \rightarrow \mathrm{CO} + 2\,\mathrm{H_2O} \tag{5}$$

$$\mathrm{C_6H_6} + \frac{9}{2}\,\mathrm{O_2} \rightarrow 6\,\mathrm{CO} + 3\,\mathrm{H_2O} \tag{6}$$

$$\mathrm{C_2H_6} + \frac{5}{2}\,\mathrm{O_2} \rightarrow 2\,\mathrm{CO} + 3\,\mathrm{H_2O} \tag{7}$$

$$\mathrm{C_2H_4} + 2\,\mathrm{O_2} \rightarrow 2\,\mathrm{CO} + 2\,\mathrm{H_2O} \tag{8}$$

$$\mathrm{CO} + \frac{1}{2}\,\mathrm{O_2} \rightarrow \mathrm{CO_2} \tag{9}$$

$$\mathrm{H_2} + \frac{1}{2}\,\mathrm{O_2} \rightarrow \mathrm{H_2O} \tag{10}$$

$$\mathrm{CO_2} + \mathrm{H_2} \leftrightarrow \mathrm{CO} + \mathrm{H_2O} \tag{11}$$

The rates of reactions are determined by the Eddy-Dissipation/Finite-Rate model (EDM/FR) which is a turbulence-chemistry interaction model that computes both the classical Arrhenius reaction rate and the turbulent mixing rate and uses the smaller of these two rates [6].

The oxidation of char (mainly composed of pure carbon) by oxygen is an exothermic process that follows this reaction [1,5]:

$$\mathrm{C} + \varphi\,\mathrm{O_2} \rightarrow (2\varphi - 1)\,\mathrm{CO_2} + 2(\varphi - 1)\,\mathrm{CO} \tag{12}$$

where φ is a char oxidation parameter defined as [3]:

$$\varphi = \frac{2 + 4.3\exp\left(-\frac{3390}{T}\right)}{2 + 8.6\exp\left(-\frac{3390}{T}\right)} \tag{13}$$

Only fuel-NOx formation is considered in this study as temperature is generally too low in wood stoves for thermal-NOx formation to occur [7]. Fuel-N (Nitrogen naturally present in the combustible) oxidation to form NOx is a complex phenomenon and normally follows both the heterogeneous and homogeneous reaction paths. In this case, only the homogeneous path is considered and the mass fraction of nitrogen in the fuel was determined by an ultimate analysis at 0.11%. Both hydrogen cyanide (HCN) and ammonia (NH_3) acts as precursors for the formation of NOx.

Soot formation is also taken into account using the Moss-Brookes model that solves two transport equations for the soot mass fraction and the normalized radical nuclei concentration

[8]. Soot particles are formed and grow by nucleation and surface growth while they decay by oxidation. In this case, ethylene is used as a precursor for nucleation and surface growth.

Regarding radiation, a multi-band approach is used due to the strong dependence of the radiative properties of the combustion products such as H_2O, CO_2 and soot. The relevant spectrum was divided into N_i=16 bands between 200 and 10 000 cm^{-1} (1 and 50 µm) in which the absorption coefficient varies with temperature and pressure [9]. In each band, the Planck-mean absorption coefficient of the combustion products $\tilde{\kappa}_{X,i}$ is defined as [10]:

$$\tilde{\kappa}_i(x,T) = \frac{\int_{\eta_i}^{\eta_i+\Delta\eta} \kappa_\eta(x,T) I_\eta^0(T)\, \mathrm{d}\eta}{\int_{\eta_i}^{\eta_i+\Delta\eta} I_\eta^0(T)\, \mathrm{d}\eta} \tag{14}$$

where η is the wave number, Δη is the band width, x denotes the combustion product (H_2O, CO_2 and soot) while I_η^0 is the black body spectral intensity at temperature T. The mean absorption coefficient $\tilde{\kappa}_i$ is defined as the sum of that of each participating medium [10], weighted by its mole fraction X:

$$\tilde{\kappa}_i(T) = X_{\mathrm{CO_2}}\tilde{\kappa}_i(\mathrm{CO_2},T) + X_{\mathrm{H_2O}}\,\tilde{\kappa}_i(\mathrm{H_2O},T) + \tilde{\kappa}_i(\mathrm{soot},T) \tag{15}$$

The radiative transfer equation is solved in each band i using the Monte-Carlo method:

$$\frac{\mathrm{d}I_i(\boldsymbol{r},\boldsymbol{s})}{\mathrm{d}s} + \tilde{\kappa}_i\, I_i(\boldsymbol{r},\boldsymbol{s}) = \tilde{\kappa}_i\, n^2\, I_\eta^0(T) \tag{16}$$

where I_i denotes the radiation intensity in the spectral band i at position $\boldsymbol{r}$ and in direction $\boldsymbol{s}$, while n is respectively the refractive index.

Finally, the source term of radiation in equation (3) is expressed as [10]:

$$-\boldsymbol{\nabla}.\boldsymbol{q_R} = \sum_{i=1}^{N_i} \tilde{\kappa}_i \int_{\eta_i}^{\eta_i+\Delta\eta} \int_0^{4\pi} I_i\,(\boldsymbol{r},\boldsymbol{s})\, \mathrm{d}\Omega - 4\pi I_\eta^0(T)\mathrm{d}\eta \tag{17}$$

where Ω is the unit solid angle.

All the previous equations were solved using ANSYS Fluent 2024R2. The drying, pyrolysis and char oxidation models were implemented using User-Defined Functions. The convergence of the simulation is assessed by the value of residuals and the stability of relevant quantities such as pressure drop, temperature and species concentrations.

3. Experiments

3.1. Biomass characterization

In order to feed the numerical model, a series of analysis of the wood pellets were carried out. A proximate analysis was realized using a Simultaneous Thermal Analyzer (STA 449 *Jupiter* – NETZSCH) to determine the moisture content, volatile matter, fixed carbon and ash content. In addition, pyrolysis gases were identified and quantified using a micro-Gas Chromatograph/Mass spectrometer (µ-GC/MC – SRA Instruments). The results of these analyses are given in Table 1 and Table 2.

Finally, the Higher Calorific Value (HCV) was measured with a bomb calorimeter (C200 – Physitek). The Lower Calorific Value (LCV) was deduced according to the ISO 18125 standard [11] and was found to be 17231 kJ/kg.

3.2. Stove instrumentation

Fifteen K-type thermocouples were introduced in the stove to measure the temperature of the gas at different locations during combustion. The flow velocity at the inlet was measured using an anemometer (PCE – THA10) and the mass flowrate was found to be 5.2 g/s. During combustion, the stove was placed on a scale to determine the devolatilization rate. The flue gases were analyzed and the concentrations of CO_2, O_2, CO, NO_x were determined and are expressed on a dry basis. From the devolatilization rate and the LCV, the heat input is 10.2 kW.

	Y (%wt)
Moisture	7.0
Volatile matter (d.b.)	79.5
Fixed carbon (d.b.)	20.3
Ash (d.b.)	0.2

Table 1: Proximate analysis of the pellets

	Y (%wt)
CO	17.4
CO_2	14.0
CH_4	3.9
H_2	0.9
H_2O	38.4
C_2H_4	0.8
C_2H_6	0.5
C_6H_6	24.1

Table 2: Composition of pyrolysis gases

4. Results

The numerical model was tested at nominal power, with the same operating parameters as the experiments. Figure 2 and Figure 3 show the temperature and oxygen contours in the stove, respectively. Combustion occurs in the crucible and above, in the combustion chamber where oxygen is quickly consumed by pyrolysis gases, producing heat. The power produced by homogeneous reactions is 7.6 kW while that of heterogeneous reactions (char oxidation) is 2.6 kW, for a total of 10.2 kW which is exactly the experimental heat input of the stove.

Figure 4 compares the numerical and the experimental temperatures measured in the crucible and in the combustion chamber along the vertical axis. An overall good accordance is noted although CFD simulations slightly overestimate temperature along the entire profile.

Similarly, the numerical model overestimates the outlet temperature of the stove, predicting 295 °C instead of the actual 269 °C. This difference probably arises from the external losses with the surrounding environment which are difficult to quantify accurately, particularly due to the uncertainties in the heat transfer coefficient and the external emissivity.

Table 3 presents a comparison between experimental and numerical results of the mole fractions of the two major compounds of the exhaust gas, CO_2 and O_2, expressed as dry basis (d.b.) and the pollutants, CO and NOx, corrected at 13% oxygen. The CFD results closely align with experiments regarding CO_2 and O_2. The CO mole fraction is marginally underestimated while the formation of NOx is correctly simulated. It is important to note that the quantity of CO is highly sensitive to fluid flow (quantity of O_2 available), temperature (reaction kinetics) but also to empirical parameters used in the EDM, which may explain the slight differences.

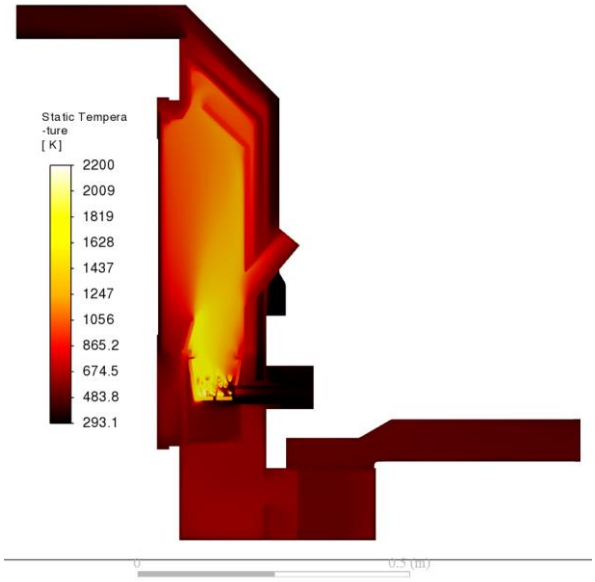

Figure 2: Temperature contours in the stove at nominal power

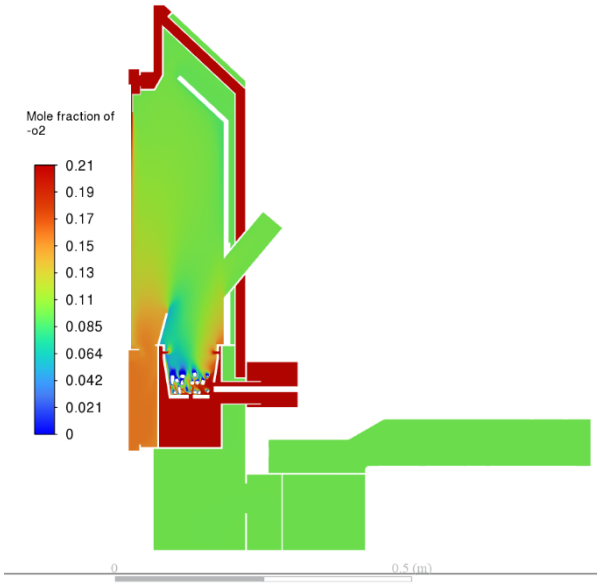

Figure 3: O_2 contours in the stove at nominal power

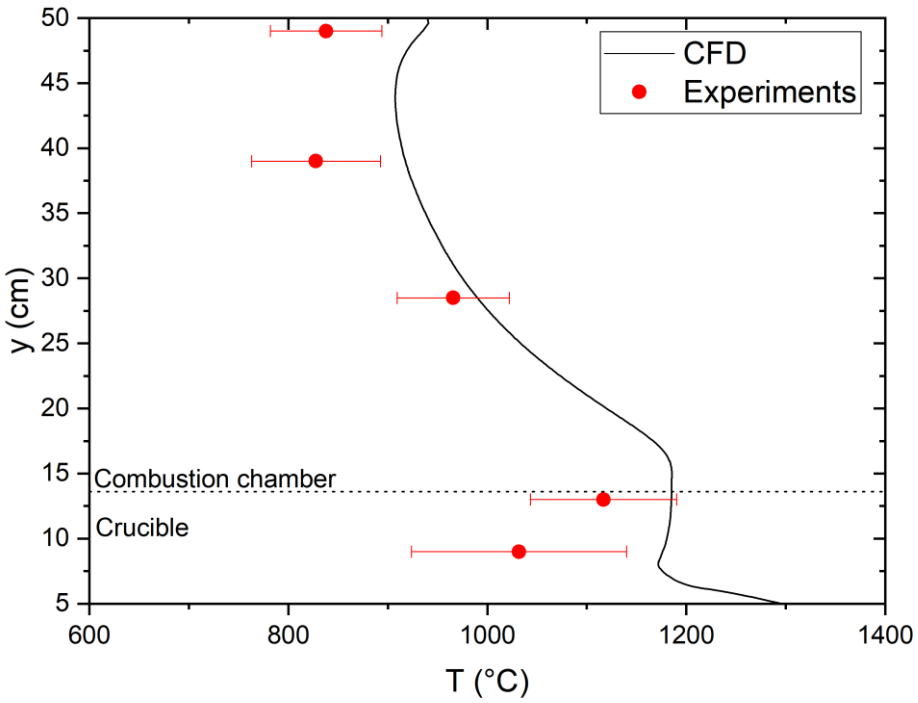

Figure 4: Comparison of experimental and numerical temperatures in the stove

	Mole fraction, d.b. (%)		Mole fraction, d.b., at 13% O_2 (ppm)	
	CO_2	O_2	CO	NOx
CFD	12.7	8.9	123	45
Experiments	12.4	8.6	144	48

Table 3: Comparison between experimental and numerical fraction of exhaust gas compounds

5. Conclusion

A 3D numerical model of a commercial pellet stove including detailed fluid flow and heat transfer with a two-step mechanism of combustion has been developed in order to predict the formation of pollutants such as carbon monoxide and nitrogen oxides. Pre-combustion phenomena, like drying of biomass and pyrolysis, as well as heterogenous reactions (char oxidation) were implemented using User-Defined Functions. A detailed multi-band radiation model was used to take into account the spectral dependency of the radiative properties of combustion products such as carbon dioxide, water vapor and soot.

A comparison of numerical results with experimental ones showed very good agreement in terms of gas concentrations (CO_2, O_2, CO and NOx) and a similar profile of temperature in the combustion chamber was observed. The model will now be used to optimize the geometry and the operating conditions of the stove to reduce the pollutant emissions.

References

[1] M.A. Gómez, J. Porteiro, D. Patiño, J.L. Míguez, CFD modelling of thermal conversion and packed bed compaction in biomass combustion, Fuel 117 (2014) 716–732. https://doi.org/10.1016/j.fuel.2013.08.078.

[2] J. Darido, A. Dhahak, R. Bounaceur, C. Le Dreff - Lorimier, G. Leyssens, F. Cazier, P. Genevray, F. Battin-Leclerc, Emissions from a Domestic Wood Heating Appliance: Experimental Measurements and Numerical Study Using an Equivalent Reactor Network (ERN) Approach Coupled with a Detailed Chemical Mechanism, Energy Fuels 35 (2021) 18680–18698. https://doi.org/10.1021/acs.energyfuels.1c01927.

[3] ANSYS, Fluent Theory Guide, (2023).

[4] F.P. Incropera, D.P. DeWitt, T.L. Bergman, A.S. Lavine, eds., Fundamentals of heat and mass transfer, 6. ed, Wiley, Hoboken, NJ, 2007.

[5] I. Haberle, Ø. Skreiberg, J. Łazar, N.E.L. Haugen, Numerical models for thermochemical degradation of thermally thick woody biomass, and their application in domestic wood heating appliances and grate furnaces, Progress in Energy and Combustion Science 63 (2017) 204–252. https://doi.org/10.1016/j.pecs.2017.07.004.

[6] B.F. Magnussen, B.H. Hjertager, On mathematical modeling of turbulent combustion with special emphasis on soot formation and combustion, Symposium (International) on Combustion 16 (1977) 719–729. https://doi.org/10.1016/S0082-0784(77)80366-4.

[7] S. Ozgen, S. Cernuschi, S. Caserini, An overview of nitrogen oxides emissions from biomass combustion for domestic heat production, Renewable and Sustainable Energy Reviews 135 (2021) 110113. https://doi.org/10.1016/j.rser.2020.110113.

[8] S.J. Brookes, J.B. Moss, Measurements of soot production and thermal radiation from confined turbulent jet diffusion flames of methane, Combustion and Flame 116 (1999) 49–61. https://doi.org/10.1016/S0010-2180(98)00027-3.

[9] W.L. Grosshandler, RADCAL - a narrow-band model for radiation calculations in a combustion environment, 0 ed., National Bureau of Standards, Gaithersburg, MD, 1993. https://doi.org/10.6028/NIST.TN.1402.

[10] J.R. Howell, M.P. Mengüç, K. Daun, R. Siegel, Thermal Radiation Heat Transfer, 7th ed., CRC Press, 2020. https://doi.org/10.1201/9780429327308.

[11] ISO 18125:2017 Solid biofuels. Determination of calorific value, 2017.